Photoalignment of Poly(di-*n*-hexylsilane) by Azobenzene Monolayer. 1. Preparative Conditions of Poly(di-*n*-hexylsilane) Spincast Film

Kazuyuki Fukuda and Takahiro Seki*

Photofunctional Chemistry Division, Chemical Resources Laboratory, Tokyo Institute of Technology, 4259 Nagatuta, Midori-ku, Yokohama, 226-8503, Japan

Kunihiro Ichimura

Research Laboratory for Science and Technology, Science University of Tokyo, 2641 Yamazaki, Noda, Chiba 278-8510, Japan

Received August 13, 2001

ABSTRACT: The photocontrol of the in-plane alignment of spincast poly(di-*n*-hexylsilane) (PDHS) film was successfully achieved on a photooriented azobenzene- (Az-) containing monolayer irradiated with linearly polarized visible light. The Si backbone of PDHS after crystallization aligned in the perpendicular direction to the polarization plane of actinic light. The preparative conditions of the PDHS film such as molecular weight of this material and thickness were examined in detail by polarized UV−visible absorption spectroscopy. The orientational order of PDHS chain was strongly dependent on the molecular weight of PDHS. Lowering of the molecular weight of PDHS gave rise to a higher orientational order of the Si backbone. With increasing film thickness, the photoalignment of the PDHS main chain became less efficient. However, successive annealing and crystallization upon cooling provided high degrees of alignment even for thicker films of the low molecular weight material. The atomic force microscopic observation revealed the formation of characteristic fibrous morphologies in the film, which was directed parallel to the electric vector of the polarization. Thus, photoinduced anisotropy in the Az monolayer controls not only the PDHS backbone alignment but also the mesoscale morphology of the film at larger hierarchies.

1. Introduction

Physical properties of polymer films such as electrical,[1] optical,[2] and mechanical[3] characteristics crucially depend on the backbone orientation, thus development of orienting method is of great importance in polymer science and technology. Chain orientations of polymer chains in thin films mostly relied on mechanical procedures including rubbing,[4] stretching,[5] friction transfer,[6] and the Langmuir−Blodgett technique.[7] An alternative candidate is epitaxial transfer from an oriented substrate surface. A variety of polymer materials can be aligned on oriented polymer surfaces,[8] prepared by stretching, rubbing, and friction deposition, and also on inorganic crystal surfaces.[9]

On the other hand, surface-mediated photoalignment has recently become an important technology in liquid crystalline materials.[10] The orientational control of polymer chains by such photochemical procedure is an alluring and challenging target because it may provide new technologies for microprocessing of polymer films. Our recent preliminary work indicated that this photochemical control is applicable also for the alignment of a polysilane, poly(di-*n*-hexylsilane) (PDHS), through the transfer from a photochemically oriented azobenzene- (Az-) containing monolayer (6Az10-PVA).[11] An illustrative presentation of the system and chemical structure of materials are shown in Scheme 1. The process investigated here presents the following two distinctive issues. First, the photoalignment of polymer main chains is performed for the first time. Second, the epitaxial growth of the chain alignment is performed on a "flexible" molecular brush, which is in contrast to conventional systems using rigid uniaxially oriented surface of polymer films[8] or inorganic crystal surfaces.[9]

Scheme 1

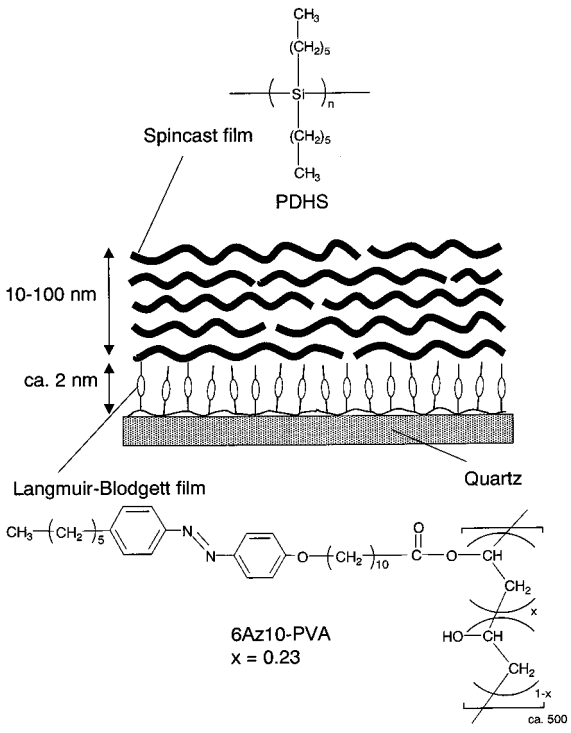

PDHS is favorably used for the observation of the polymer organizations because simple UV−visible absorption spectral measurements provide useful information on both conformational and orientational states of

* To whom correspondence should be addressed. Fax: +81−45−924−5247. E-mail: tseki@res.titech.ac.jp.

10.1021/ma0114584 CCC: $22.00
Published on Web 02/09/2002

the backbone due to the delocalization of the σ-electron along the catenated Si chain.[12] The PDHS film shows a reversible conformational transition, which is reflected in the light absorption property. PDHS has an absorption maximum at ca. 370 nm at room temperature. Above 42 °C, the absorption peak shifts to ca. 320 nm. This is due to a conformational change of the Si backbone and the molecular packing state from an ordered phase (crystalline phase) to a disordered one (columnar mesomorphic phase).[12,13]

We have reported some preliminary results on the alignment behavior of PDHS on a photoaligned Az monolayer by linearly polarized light (LPL);[11] however, detailed factors affecting the PDHS alignment have not been elucidated. Parameters affecting the photoalignment may be classified into two categories: factors relating to the preparative conditions of the PDHS film and factors relating to the design of the Az monolayer on the substrate. This paper focuses to the effects of preparative conditions of the PDHS film in terms of the molecular weight of PDHS and the thickness of the spincast film. Detailed examinations relating to the molecular design and preparative control of the Az monolayer on the substrate surface will be described in a subsequent report.[14]

2. Experimental Section

2.1 Materials. The synthetic procedure for 6Az10-PVA was described in the previous report.[15] PDHS was prepared by reductive condensation of the dihexyldichlorosilane (Chisso Ltd.) with sodium metal in dry toluene.[12,16] The molecular weight was determined by gel permeation chromatography (GPC) analysis (JASCO Intelligent UV/vis detector 875-UV with Integrator 807-IT) using polystyrene as the calibration standard. PDHS materials of three different molecular weights ($M_w = 1.4 \times 10^6$, $M_w/M_n = 1.9$; $M_w = 3.1 \times 10^5$, $M_w/M_n = 2.1$; $M_w = 2.5 \times 10^4$, $M_w/M_n = 2.7$) were prepared by solvent fractionation from toluene, using 2-propanol and methanol as the poor solvent.

Fused silica plates were cleaned with a saturated potassium hydroxide/ethanol and then ethanol followed by washing with pure water (Milli-Q).

2.2. Preparation of PDHS Films on Az Monolayer. A photochromic monolayer of Az containing amphiphilic polymer (6Az10-PVA) was first transferred onto a fused silica plate by the Langmuir−Blodgett (LB) method.[17] A chloroform solution containing 6Az10-PVA (1.0×10^{-3} mol dm^{-3}) was preirradiated with UV light (365 nm from a Hg−Xe lamp) for 5 min to allow the *cis*-Az-rich photostationary state. This 6Az10-PVA solution was spread on pure water (Milli-Q) filled in a LAUDA FW−II film balance at 20 °C. After evaporation of the solvent, the monolayer was compressed at a speed of 1.0 cm min^{-1}. The *cis*-6Az10-PVA monolayer was transferred onto a fused silica substrate at 0.4 nm^2 per Az unit by standard vertical lifting at 0.2 cm min^{-1}. The transfer ratio was virtually unity. The deposition in the cis form is a requirement from the preparation of a highly homogeneous 6Az10-PVA LB monolayer on the substrate. The deposited monolayer was stored in the dark to allow thermal isomerization to the trans form of Az.[18]

The stored 6Az10-PVA films was first irradiated with nonpolarized 365 nm light 0.3 J cm^{-2} to enrich the *cis*-Az content and then irradiated with LPL at 436 nm (3.0 J cm^{-2}). This irradiation procedure led to a high degree of orientation of Az in the in-plane component. PDHS films were prepared on the top of the orientated Az monolayer by spincasting from hexane solutions. It was confirmed spectroscopically that the contact with hexane solution does not disturb the photoinscribed structure of the Az monolayer. The thickness of the PDHS film was controlled by adjusting the concentration of PDHS/hexane solution.

2.3. Measurements. UV−visible absorption spectra were taken on a Hewlett-Packard diode array spectrometer 8452A or a JASCO model MAC-1 spectrometer that is suited for weakly absorbing samples. The accuracy of absorbance with this instrument reached a level of 1.0×10^{-4}. For polarized spectra, a polarizer mounted in a rotating holder was placed in front of the samples.

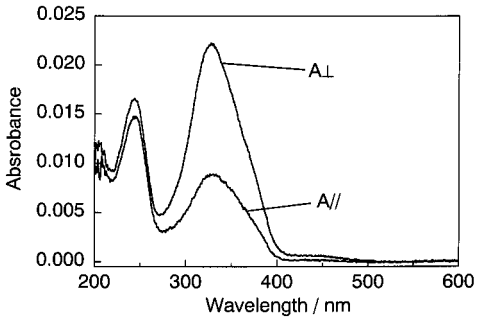

Figure 1. Polarized UV−visible absorption spectra of the 6Az10-PVA monolayer irradiated with LPL at 436 nm. The spectra were taken with a polarized probe beam at perpendicular ($A_\perp$) and parallel ($A_{||}$) directions relative to the polarization plane of actinic light.

The light irradiation was performed with a 150 W Hg−Xe lamp (San-ei UV supercure-230S) combined with optical filters for wavelength selection (Toshiba optical filters UV-35/UV-D36A for 365 nm illumination, and Y-43/V-44 for 436 nm illumination).

Film thickness of the initial PDHS film was estimated by surface profilometry using a Dektak^{3}ST (ULVAC/Sloan Co.) The film was scratched, and the height difference between the substrate surface and the film surface was measured. Averages of more than three measurements were adopted for the value of film thickness.

The FTIR spectra were recorded on a Biorad FTS6000 spectrometer equipped with a DTGS detector. The system was purged with dried air. A CaF_2 plate was used as the substrate for the transmission measurement. A polarizer (JEOL IR-Opt02) was placed in front of the sample, and the measurement was carried out in the normal incidence.

Atomic force microscopic (AFM) images were taken with a Seiko SPA300/SPI3700 system in the dynamic force mode at an ambient atmosphere. A micro-cantilever of SI-DF20 (20 μm scanner, a rectangular-shaped Si tip) was used. The spring constant was 13 N m^{-1}, and the resonance frequency was 130 kHz according to the manufacturer. The scan speed was 0.5−1.0 Hz.

3. Results and Discussion

3.1. Photoalignment of PDHS. Alignment of the Si Backbone. Figure 1 shows the polarized absorption spectra of the 6Az10-PVA monolayer after irradiation with LPL at 436 nm. Exposure of the LPL to the monolayer induced the orientation of Az moiety preferentially in the perpendicular direction to the polarization plane of actinic light with respect to the in-plane component. The electric vector of the polarized light induced a molecular reorientation to a nonexcitable direction.[19] In the present case, the dichroic ratio $[(A_\perp - A_{||})/(A_\perp + A_{||})]$ was 0.42.

A spincast film of PDHS ($M_w = 2.5 \times 10^4$, film thickness = 45 nm) was subsequently prepared onto this Az monolayer. In these experiments, the PDHS having the lowest molecular weight was employed. Figure 2 shows the polarized absorption spectra of PDHS film. Immediately after spincasting, the PDHS film was fully in a mesophasic (disordered) phase (316 nm absorption) and had no optical anisotropy (Figure 2a). Storage of the PDHS film in the dark at room temperature for 2 days allowed a sufficient crystallization (360 nm absorption). After crystallization, the PDHS film exhibited an

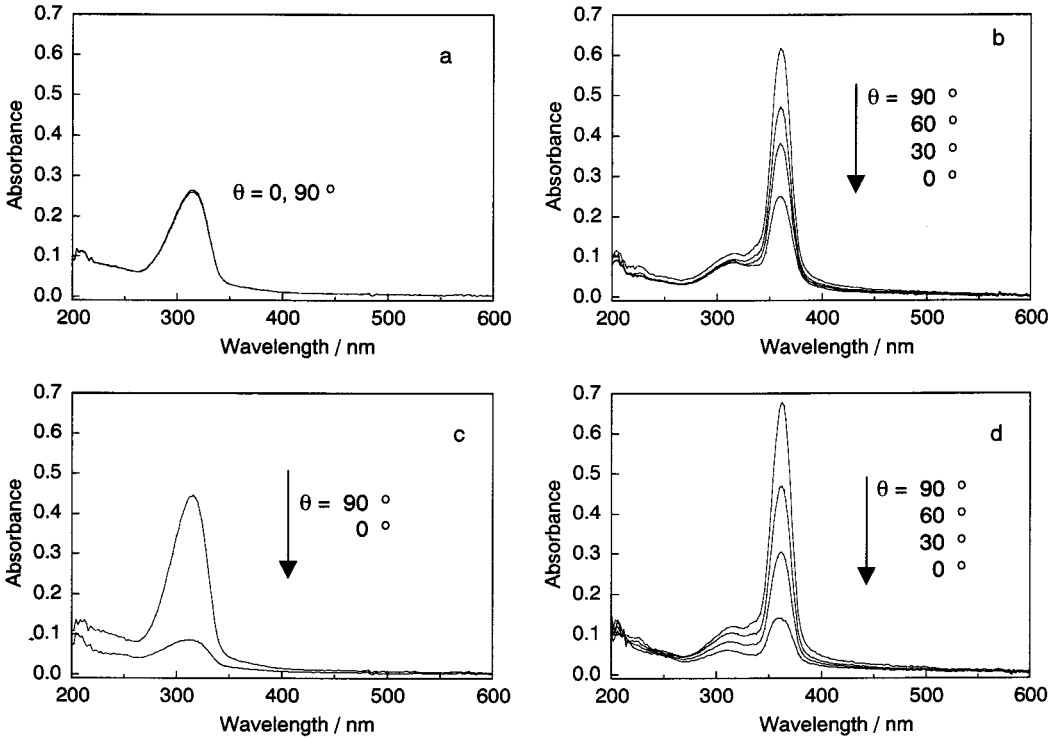

Figure 2. Polarized UV−visible absorption spectra of a PDHS ($M_w = 2.5 \times 10^4$) film on the 6Az10-PVA monolayer irradiated with LPL at 436 nm. The spectra were taken with a polarized probe beam at an angle θ relative to the polarization plane of actinic light. The spectra were immediately taken after spincasting (a) and crystalliziation at room temperature for 2 days (b). Furthermore, the PDHS film was annealed at 100 °C for 1 h (c) and then crystallized again (d).

in-plane anisotropic nature (Figure 2b). As shown, the polarized absorption spectra revealed that the Si main chain is aligned perpendicular to the polarization plane of the actinic light. The aligned direction of the PDHS main chain agreed with that of the Az orientation on the substrate. This fact indicates that the crystallization of the PDHS chain occurred on the photooriented Az monolayer in an epitaxial manner. It seems that an initial local anisotropic nucleation in the vicinity of the oriented Az layer governs the alignment of the whole film after crystallization. The enhancement of the absorbance after crystallization is attributed to an increased molar extinction coefficient for the more extended chain.[20]

The orientational order of PDHS film was further enhanced upon annealing and successive cooling. The order parameter, S [$=(R-1)/(R+2)$, where R = abs(90°)/abs(0°)], evaluated for the ordered phase was 0.33 before annealing (Figure 2b). When this film was annealed at 100 °C for 1 h, the intensity of the peak around 316 nm corresponding to the disordered phase increased, and the peak around 360 nm thoroughly disappeared. Thus, the annealing procedure gave the complete transition to the conformationally disordered phase.[12] In this case, the PDHS chain alignment was enhanced to a higher order ($S = 0.58$, Figure 2c).

Successive cooling of this sample to room temperature gave a crystalline film with an orientational order of $S = 0.56$ and higher crystallinity (Figure 2d). Lovinger et al.[21] reported that the lateral packing correlation of the disordered part is improved by heating above the transition temperature (42 °C), and the regenerated crystalline phase after cooling shows an increased orientational order. The same tendency was observed in the present work. The annealing temperature adopted here (100 °C) was not a special requirement. The orientational enhancement was also induced fully after annealing at a lower temperature slightly above the transition temperature (50 °C).

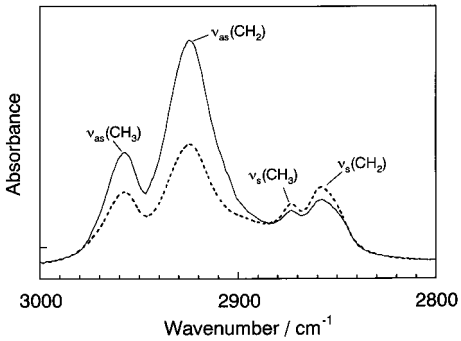

Figure 3. Polarized IR spectra of the aligned PDHS ($M_w = 2.5 \times 10^4$) film on Az monolayer. Solid and dashed lines represent the spectra taken at perpendicular and parallel to the polarization plane of actinic light.

The increase in the orientational order was hardly observed upon further annealing and cooling. Once the PDHS chain was aligned, the alignment was strongly memorized and fixed. Irradiation with LPL with a different polarization direction did not alter the direction of the PDHS chain.

Orientation of the Hexyl Side Chain. IR spectroscopy provides information on the orientation of alkyl chain. Figure 3 shows the polarized transmission FTIR spectra in the wavenumber regions of methyl ($-CH_3$) and methylene ($-CH_2-$) vibrations for a photoaligned PDHS film. The absorption of the bands at 2925 and 2856 cm^{-1} are assigned to the asymmetric and symmetric CH_2 stretching bands, respectively. The peak positions are indicative of the involvement of gauche conformers.[22,23] Thus, the crystalline state is somewhat

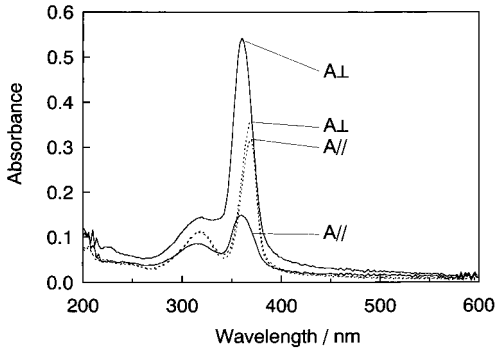

Figure 4. Polarized UV−visible absorption spectra of PDHS films crystallized on the photooriented 6Az10-PVA monolayer preirradiated with LPL at 436 nm. The molecular weights of PDHS were 1.4×10^6 (dash line) and 2.5×10^4 (solid line).

Table 1. Spectral Features of Photooriented PDHS Films: Absorption Peak Position λ_{max} and Orientational Order Parameter[a]

		S	
mol wt	λ_{max}/nm	1st cryst	2nd cryst
2.5×10^4	360	0.47	0.56
3.1×10^5	368	0.10	0.15
1.4×10^6	368	0.04	0.04

[a] Film thickness = 35-40 nm.

disordered. These bands indicated an anisotropic nature. For the asymmetric band, the absorbance obtained with the perpendicular probing polarization to the actinic LPL was larger than that with the parallel direction; the opposite tendency was found for the symmetric one. Since the transition moments of the two bands are orthogonal to each other and are perpendicular to the alkyl side chain axis, this fact gives a model where the hexyl side chains are aligned perpendicular to each other with respect to the substrate surface. This knowledge is in consistent with the rubbing induced alignment of PDHS as studied by Tachibana et al.[4] Therefore, the structural feature of the photoaligned PDHS resembles that obtained by the rubbing method.

3.2. Effects of the Molecular Weight. The long-chain nature of polymers in general prevents a sharp alignment of polymer crystals in the epitaxial growth process.[24] In this respect, PDHS materials having three different molecular weights [$M_w = 2.5 \times 10^4$ (M_w/M_n = 2.7), $M_w = 3.1 \times 10^5$ (M_w/M_n = 2.1), and $M_w = 1.4 \times 10^6$ (M_w/M_n = 1.9)] were employed in order to clarify the influences of molecular weight on the photoorienting behavior.

Figure 4 shows the UV absorption spectra of the photoaligned PDHS films having the lowest ($M_w = 2.5 \times 10^4$) and the highest ($M_w = 1.4 \times 10^6$) molecular weight prepared on the photoaligned Az monolayer. The spectra were taken after sufficient crystallization. As shown, the difference in the molecular weight did not affect the orienting direction; however, the degree of orientational order was markedly influenced.

Table 1 summarizes the order parameter (*S*) and the peak position (λ_{max}) of the ordered phase obtained from UV absorption spectral data. The PDHS having the lower molecular weight gave the higher in-plane orientational order. The PDHS with lower molecular weight leads to a sharper epitaxial alignment, probably due to more degrees of allowed segmental freedom with less entanglement or less physical cross-linking. The orientational order and crystallinity were enhanced after

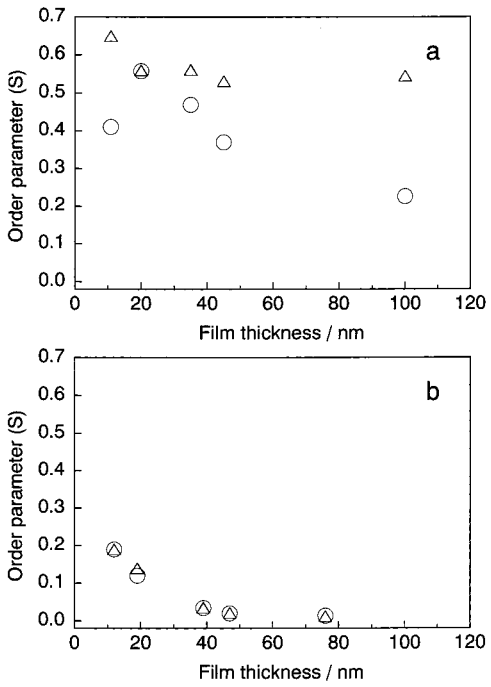

Figure 5. Orientational order parameter (*S*) of PDHS films as a function of film thickness. The circle and triangle represent data after the first and second crystallization, respectively. M_w of PDHS were 2.5×10^4 (a) and 1.4×10^6 (b).

successive annealing and cooling (second crystallization), which was again dependent on the molecular weight. *S* of PDHS film of the lowest molecular weight (2.5×10^4) was enhanced from 0.47 to 0.56 after the second crystallization. The improvement of *S* was minor for the intermediate molecular weight sample ($M_w = 3.1 \times 10^5$), *S* changing from 0.10 to 0.15. For the sample of the highest molecular weight ($M_w = 1.4 \times 10^6$), no enhancement in *S* was observed ($S = 0.04$). The prevention of the orientational improvement in the second crystallization for the higher molecular weight material can be resulted possibly from two factors. One is the suppressed segmental freedom of polymer chains as mentioned for the first crystallization. Another factor can be the small degree of orientational order after the first crystallization, which results in an insufficient improvement of alignment on annealing. The former interpretation is more plausible since no improvement in *S* was observed for properly aligned thinner films (thickness below 20−30 nm) of the highest molecular weight sample (see section 3.3).

The absorption maximum also changed with variations in the molecular weight of PDHS. The absorption maximum of PDHS films of $M_w = 2.5 \times 10^4$, 3.1×10^5, and 1.4×10^6 were positioned at 360, 368, and 368 nm, respectively. The bathochromic shift of the UV absorption peak observed in the high molecular weight PDHS films shows the more effective σ-electron delocalization in the PDHS backbone. These results indicate that PDHS having the lowest molecular weight led to the highest in-plane orientational order in total, but the conjugation state of the main chain is the less ordered.

3.3 Effects of Film Thickness of PDHS. Since the in-plane-component orientation of the Az monolayer should initially affects the PDHS chain in the contacting region, the orientational order of the entire film seems to be dependent on the film thickness. Furthermore, Despotopoulou et al.[25] showed a large effect of film

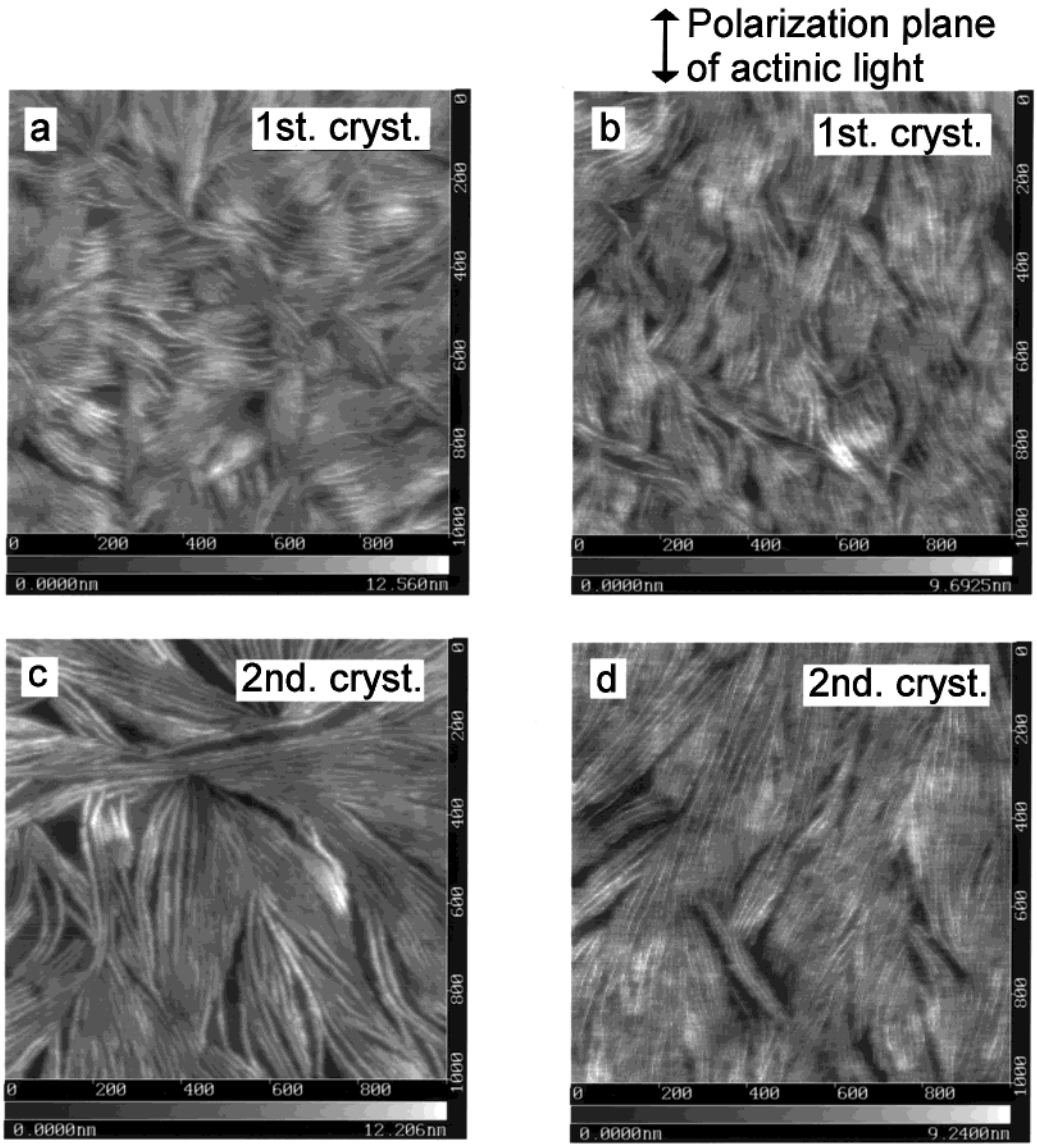

Figure 6. Topographical AFM images of PDHS ($M_w = 2.5 \times 10^4$) films on the Az monolayer without irradiation (a and c) and preirradiated with LPL (b and d). The average film thickness was 20 nm. The images were taken after the first crystallization (a and b) and second crystallization (c and d).

thickness on the crystallization behavior of PDHS below 50 nm. It is therefore of significance to conduct an exploration on the thickness dependence for understanding the photoalignment behavior of PDHS.

A PDHS film with varied thickness from 10 to 100 nm was prepared on the preirradiated Az monolayer. Figure 5 shows the order parameter (S) as a function of film thickness for the PDHS films of the lowest molecular weight ($M_w = 2.5 \times 10^4$) (a) and the highest one ($M_w = 1.4 \times 10^6$) (b). In both cases, the orientational order of the PDHS backbone became larger for the thinner films (circles in a and b).

The order parameter was enhanced after the second crystallization for the lower molecular weight sample (triangles in Figure 5a). The orientational order was enhanced upon annealing and the S for thicker films became comparable with those of the thinner ones. It can be reasonably assumed that the influence of the photooriented Az layer did not reach the overall thickness after just the first crystallization. However, the lateral packing correlation of the disordered part was improved by heating, leading to an enhancement of orientational order at least within thicknesses less than 100 nm.

In the case of the high molecular weight material, the photoalignment of PDHS was largely suppressed (Figure 5b). When the PDHS film became thicker than 30 nm, essentially no alignment in the PDHS chain was induced. The photoalignment effect was observed for the thinner films having less than 20 nm thickness, however, the alignment was quite insufficient, S being less than 0.2. No enhancement in S was observed even after annealing. The significant influence of the epitaxial alignment was admitted at thicknesses below 30 nm, which is almost in accord with the knowledge on the two-dimensional constraint of PDHS films as demonstrated by Frank's group.[25]

3.4. Morphologies Observed by Atomic Force Microscopy. 3.4.1 Morphological Features. The surface morphologies of the PDHS ($M_w = 2.5 \times 10^4$, the lowest molecular weight) films were observed by AFM. Figure 6 shows the topographical AFM images of PDHS films formed on a nonirradiated (a and c) and LPL-irradiated (b and d) Az monolayer. Here, the average

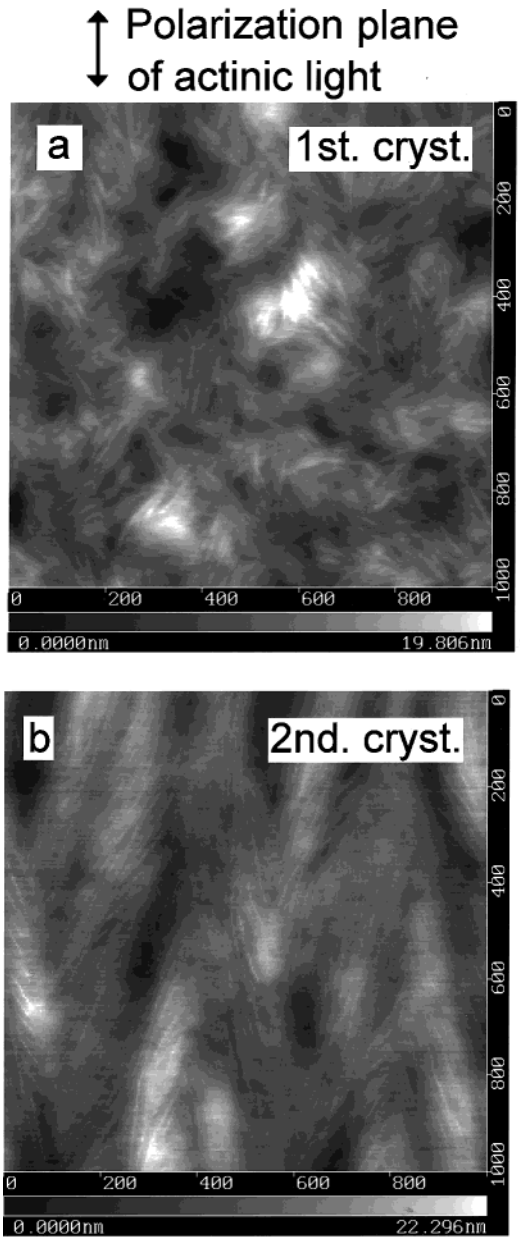

Figure 7. Topographical AFM images of PDHS ($M_w = 2.5 \times 10^4$) film on the Az monolayer preirradiated with LPL. The average film thickness was 100 nm. The images were taken after the first crystallization (a) and second crystallization (b).

film thickness of PDHS was 20 nm for the both samples. The films were prepared by spincasting and were crystallized at room temperature for 1 day.

Characteristic fibrous patterns were observed in topographical images in both cases. The fibrous patterns formed on the photooriented Az monolayer were preferentially aligned parallel to the polarization plane of actinic light (Figure 6b). In appearance, the fibers grew up to ca. 200 nm in length and ca. 13 nm in width (uncorrected for the AFM cantilever width). The thickness in the *z* direction of the fiber ranged 3−7 nm. As described in section 3.1, the PDHS Si backbone is preferentially aligned perpendicular to the polarization direction, and thus the Si backbone and the fibers are directed perpendicular to each other. It is therefore implied that the PDHS chain is folded orthogonal to the fibrous structure. AFM images indicates that the fibers are gathered to form sheaflike bundles. The fibrous structure was also observed for a PDHS film formed on a nonirradiated Az monolayer (Figure 6a). In this case, the fibers are aligned at local scales, but the direction was not controlled over the whole area. The dimensions of the finest fibrous structure in terms of length width and height were the same as those of the photoaligned organization.

After the second crystallization, the fibrous structures became clearly elongated (nearly to several nanometers level) in both cases on the nonirradiated (Figure 6c) and LPL irradiated (Figure 6d) Az monolayers. This reasonably agrees with the knowledge of the promoted crystallization after second crystallization.

Most probably, the PDHS backbone is folded to form a lamella structure, and the lamella is elongated to the polarization plane direction. The formation of the fibrous structure was characteristics of the low molecular weight sample (M_w in the range of 10^4). The high molecular weight PDHS above M_w of 10^5 did not form fibers. It is to be stressed that the Az monolayer controls not only the alignment of the Si backbone but further the film morphology of higher hierarchies.

3.4.2. Annealing Effect in a thicker film. Figure 7 shows the topographical AFM images of PDHS films of average thickness of 100 nm on preirradiated Az monolayer after the first crystallization (Figure 7a) and the second one (Figure 7b). Fibrous structures were observed also for this thicker PDHS film, however, the direction of the fibers was not controlled before annealing. After annealing and successive crystallization (second crystallization), the fibers were evidently aligned along the polarization direction of the actinic light in a similar manner as observed for the thinner film. The thicker film exhibits hierarchical organizations in which the fibers were assembled to form sheaflike larger bundles having widths of several tens of nanometers. The morphological change in the thicker film after the second crystallization can be explained as follows. After the first crystallization before annealing, the photoorientation is attained only in the vicinity of the oriented Az surface. The orientational control of the PDHS in the entire region is just attained after the second crystallization process, leading to the appearance of the anisotropic morphology on the surface. This interpretation reasonably explains the larger increase in *S* for the thicker films after the second crystallization, and also the saturated magnitude of *S* after the second crystallization for samples of any thickness examined (Figure 5a).

4. Conclusions

As shown in the present study, the photoalignment behavior of PDHS significantly depends on the preparative conditions of PDHS. Data presented here obviously indicate that the orientational order of the Si backbone and the conformation depend on the molecular weight and the film thickness. The annealing and successive second crystallization highly improves the in-plane alignment for the low molecular weight material, however, no effect was admitted for the high molecular one. It is probable that chain entanglement among the polymer chain impedes the alignment for the high molecular weight PDHS. Photoalignment of PDHS by the Az monolayer is efficient in the thickness ranges below 30 nm for the first crystallization. These values are in good agreement with the data of Despotopoulou et al.[25] describing that the modifications on the crystallization behavior becomes prominent at this thickness

level. Therefore, the consistency in the film thickness strongly implies that the present photoassisted phenomena are strongly coupled with the intrinsic organization of the PDHS.

The Az monolayer controls not only the alignment of the Si backbone but also the film morphology of higher hierarchies. Thus, knowledge about the lamella formation process may be essential to understand the alignment behavior of PDHS. Detailed investigation in this aspect is now in progress.

This paper dealt with only the factors of the PDHS film preparation. The alignment behavior should be strongly influenced by the design of the surface Az monolayer. Investigation in this aspect will be presented in the following paper.[14] We anticipate that the photoalignment of polymer is not limited to PDHS but may be extended to other polymers including π-conjugated systems.

Acknowledgment. We thank Drs. S. Morino, M. Nakagawa, K. Arimitsu, and T. Ubukata for their helpful discussions. This work was financially supported by a Grand-in-Aid for Scientific Research on Priority Areas, "Molecular Synchronization for Design of New Materials System," and a Grand-in-Aid for Scientific Research (13875188 to T.S.) from the Ministry of Education, Science, Sports, and Culture, Japan, and the NISSAN Science Foundation.

References and Notes

(1) Cao, Y.; Smith, P.; Heeger, A. J. *Polymer* **1991**, *32*, 1210.
(2) (a) For a comprehensive overview, see: Michl, J.; Thulstrup, E. W. *Spectroscopy with Polarized Light*; VCH: New York, 1986. (b) Grell, M.; Baradley, D. D. C. *Adv. Mater.* **1999**, *11*, 895.
(3) (a) Smith, P.; Lemstra, P. J. *J. Mater. Sci.* **1980**, *15*, 505. (b) Capaccio, G.; Crompton, T. A.; Ward, M. *J. Polym. Sci., Polym. Phys. Ed.* **1976**, *14*, 1641.
(4) Tachibana, H.; Matsumoto, M.; Tokura, Y. *Macromolecules* **1993**, *26*, 2520.
(5) Harrah, L. A.; Zeigler, J. M. *Macromolecules* **1987**, *20*, 601.
(6) Tanigaki, N.; Yase, K.; Kaito, A.; Ueno, K. *Polymer* **1995**, *36*, 2477.
(7) (a) Embs, F. W.; Wegner, G.; Neher, D.; Albouy, P.; Miller, R. D.; Wilson, C. G.; Schrepp, W. *Macromolecules* **1991**, *24*, 5068. (b) Nakano, Y.; Murai, S.; Kani, R.; Hayase, S. *J. Polym. Sci., Part A: Polym. Chem.* **1993**, *31*, 3361. (c) Seki, T.; Tamaki, T.; Ueno, K. *Macromolecules* **1992**, *25*, 3825.
(8) (a) Wittmann, J. C.; Lotz, B. *Prog. Polym. Sci.* **1990**, *15*, 909. (b) Wittmann, J. C.; Smith, P. *Nature* **1991**, *352*, 414.
(9) Mauritz, K. A.; Bear, E.; Hopfinger, A. J. *J. Polym. Sci., Macromol. Rev.* **1978**, *13*, 1.
(10) Ichimura, K. *Chem. Rev.* **2000**, *100*, 1847. (b) O′Neill, M.; Kelly, S. M. *J. Phys. D: Appl. Phys.* **2000**, *33*, R67.
(11) Seki, T.; Fukuda, K.; Ichimura, K. *Langmuir* **1999**, *15*, 5098.
(12) Miller, R. D.; Michl, J. *Chem. Rev.* **1989**, *89*, 1359.
(13) Miller, R. D.; Hofer, D.; Rabolt, J.; Fickes, G. N. *J. Am. Chem. Soc.* **1985**, *107*, 2172.
(14) Part 2 of this series: Fukuda, K.; Seki, T.; Ichimura, K. *Macromolecules* **2002**, *35*, 1951.
(15) (a) Ichimura, K.; Suzuki, Y.; Seki, T.; Kawanishi, Y.; Aoki, K. *Makromol. Chem. Rapid Commun.* **1989**, *10*, 5. (b) Seki, T.; Sakuragi, M.; Kawanishi, Y.; Suzuki, Y.; Tamaki, T.; Fukuda, R.; Ichimura, K. *Langmuir* **1993**, *9*, 211.
(16) Rabolt, J.; Hofer, D.; Miller, R. D.; Fickes, G. N. *Macromolecules* **1986**, *19*, 611.
(17) Seki, T.; Ichimura, K. *Thin Solid Films* **1989**, *179*, 77.
(18) The deposited monolayer was stored in a dry atmosphere to allow the cis-to-trans thermal isomerization since the morphology of 6Az10-PVA monolayer after the thermal isomerization is strongly dependent on the humidity of the atmosphere. For the films stored in a highly humidified atmosphere, lateral film contraction was observed in the film morphology. On the other hand, a molecularly flat film that preserved the initial state was observed for the film stored in a dry atmosphere: Seki, T.; Kojima, J.; Ichimura, K. *Macromolecules* **2000**, *33*, 2709.
(19) (a) Stumpe, J.; Fischer, Th.; Menzel, H. *Macromolecules* **1996**, *29*, 2831. (b) Stumpe, J.; Geue, Th.; Fischer, Th.; Menzel, H. *Thin Solid Films* **1996**, *284*, 606. (c) Fischer, Th.; Menzel, H.; Stumpe, J. *Supramol. Sci.* **1997**, *4*, 543. (d) Geue, Th.; Ziegler, A.; Stumpe, J. *Macromolecules* **1997**, *30*, 5729.
(20) Fujiki, M.*J. Am. Chem. Soc.* **1996**, *118*, 7424.
(21) (a) Lovinger, A. J.; Schilling, F. C.; Bovey, F. A.; Zeigler, J. M. *Macromolecules* **1986**, *19*, 2657. (b) Kyotani, H.; Shimomura, M.; Miyazaki, M.; Ueno, K. *Polymer* **1995**, *36*, 915.
(22) Sapper, H.; Cameron, D. G.; Mantsch, H. H. *Can. J. Chem.* **1981**, *59*, 2543.
(23) Katayama, N.; Ozaki, Y.; Seki, T.; Tamaki, T.; Iriyama, K. *Langmuir* **1994**, *10*, 1898.
(24) Isoda, S. *Polymer* **1984**, *25*, 615.
(25) (a) Frank, C. W.; Rao, V.; Despotopoulou, M. M.; Pease, R. F. W.; Hinsberg, W. D.; Miller, R. D.; Rabolt, J. F. *Science* **1996**, *273*, 912. (b) Despotopoulou, M. M.; Frank, C. W.; Miller, R. D.; Rabolt, J. F. *Macromolecules* **1996**, *29*, 5797. (c) Despotopoulou, M. M.; Miller, R. D.; Rabolt, J. F.; Frank, C. W. *J. Polym. Sci., Part B: Polym. Phys.* **1996**, *34*, 2335.

MA0114584